RESEARCH

ESTIMATING MONTHLY SOLAR RADIATION IN SOUTH-CENTRAL CHILE

José Álvarez[1*], Helena Mitasova[2], and H. Lee Allen[1]

Solar radiation is a key component in process-based models. The amount of this energy depends on the location, time of the year, and atmospheric conditions. Several equations and models have been developed for different conditions using historical data from weather station networks or satellite measurements. However, solar radiation estimates are too local since they rely on weather stations or have a resolution that is too coarse when working with satellites. In this study, we estimated monthly global solar radiation for the south-central region of Chile using the *r.sun* model and validated it with observations from automatic weather stations. We analyzed the performance of global radiation results with the Hargreaves-Samani (HS) and Bristow-Campbell (BC) models. Estimates from a calibrated *r.sun* model accounted for 89% of the variance (r^2 = 0.89) in monthly mean values for 15 locations in the research area. The model performed very well for a wide area and conditions in Chile when we compared it with the HS and BC models. Our estimates of global solar radiation using the *r.sun* model could be improved through calibration of ground measurements and more precise cloudiness estimates as they become available. With additional procedures, the *r.sun* model could be used to provide spatial estimates of daily, weekly, monthly, and yearly solar radiation.

Key words: Solar radiation, *r.sun* model.

Soil and climatic conditions in the south-central region of Chile favor the production of numerous crops, including wheat, fruits, and timber. Crop productivity is highly correlated with climatic conditions (solar radiation, amount and distribution of rainfall, and temperature). This area generally has a Mediterranean climate with dry summers. However, climatic conditions can vary dramatically over short distances due to the effects of the Pacific Ocean and the Coastal and Andes Mountains (Díaz *et al*., 2010). To predict productivity under these conditions, climatic data are essential. Several process-based models, such as 3-PG (Landsberg and Waring, 1997; Coops *et al*., 1998; Tickle *et al*., 2001; Sands and Landsberg, 2002; Almeida *et al*., 2004; Stape *et al*., 2004), Biomass (McMurtrie *et al*., 1990), Cabala (Battaglia *et al*., 2004), and Maestro (Wang and Jarvis, 1990), use climate, soil, and physiological parameters as input variables. Solar radiation is the driver variable for all these models.

Process-based models have not been widely used in Chile due to the lack of solar radiation data. Several efforts have been made to predict global radiation in Chile (Meza and Varas, 2000; Yilmaz *et al*., 2007) but only for specific locations and not over wide regions. Because of the gap between the need for and availability of irradiation data, several options have been developed to predict solar radiation with mechanistic models using recorded meteorological data (Kermel, 1988; Bindi and Miglietta, 1991; Muneer *et al*., 2000; Coops *et al*., 2000; Almeida and Landsberg, 2003; Ball *et al*., 2004), remote sensors (Cano *et al*., 1986; Diabate *et al*., 1989; Garatuza-Payan *et al*., 2001; Suri and Hofierka, 2004; Lefevre *et al*., 2007), or geophysical calculations with the solar constant and discount of transmissivity through the atmosphere (Suri and Hofierka, 2004; Ball, 2004). The latter models have been used in Europe (Hofierka and Suri, 2002; Romero *et al*., 2008), in specific locations in Chile (Yilmaz *et al*., 2007), and in the United States (Ball *et al*., 2004).

During the last two decades, the availability of more powerful computer hardware and geographical information systems (GIS) has been significant in the development of solar radiation model modules (Suri and Hofierka, 2004). More advanced methods for ecological and biological applications are used in *Solar Analyst*, developed as an ArcView GIS extension module. This is based on the DEM (Digital Elevation Model), a model which generates an upward-looking hemispherical viewshed. These types of models, integrated with GIS, provide rapid, cost-efficient, and accurate estimates of solar radiation over large territories taking into account surface inclination, aspect, and shadowing effects (Hofierka and Suri, 2002).

A relatively new approach called the *r.sun* module (Suri and Hofierka, 2004) implemented under an open source GRASS GIS environment (Neteler and Mitasova, 2008) has provided a more flexible and spatially explicit tool to

[1]North Carolina State University, Department of Forestry and Environmental Resources, Raleigh, North Carolina, USA. [*]Corresponding author (jsmunoz@ncsu.edu).
[2]North Carolina State University, Department of Marine, Earth and Atmospheric Sciences, Raleigh, North Carolina, USA.
Received: 5 January 2011.
Accepted: 23 August 2011.

estimate solar radiation. This open-source implementation allows for future improvements and applications.

The *r.sun* model estimates global radiation under clear-sky conditions from the sum of its beam, diffuse, and reflected components for a given day, latitude, surface, and atmospheric conditions. While the calculation of the beam component is quite straightforward, the main difference between the various models is how the diffuse component is treated. This component depends on climate and regional terrain conditions, and it is often the largest source of estimation error (Hofierka and Suri, 2002).

The *r.sun* algorithm uses equations published in the European Solar Radiation Atlas (ESRA, 2000). Global horizontal radiation is calculated with the Linke turbidity index (Linke, 1922) T_{LK}, which describes the atmosphere's optical thickness due to both water vapor absorption and aerosol particle absorption and scattering in relation to the dry and clean atmosphere, and the *r.sun* module in GRASS (http://grass.fbk.eu/) integrating the beam and diffuse components (Hofierka and Suri, 2002):

$$G_{hc} = B_{hc} + D_{hc} \quad [1]$$

where G_{hc} is the global horizontal radiation, B_{hc} is direct radiation, and D_{hc} is diffuse radiation.

The *r.sun* model considers the Earth's geometry, revolution, and rotation, which are factors that determine the available extraterrestrial radiation based on solar position above the horizon and can be precisely calculated with astronomic formulas.

The radiation input to the Earth's surface is then modified by the slope inclination and aspect, as well as the shadowing effects of neighboring terrain features. These factors can be modeled at a high accuracy level. The elevation above sea level determines the attenuation of radiation by the atmosphere's thickness. The intensity of the extraterrestrial solar radiation traversing the Earth's atmosphere is attenuated by various atmospheric constituents, such as gases, liquid and solid particles, and clouds. The path length through the atmosphere is also critical.

The theoretical background and applications are described in a paper by Suri and Hofierka (2004). More details about the model can be consulted in the *r.sun* manual (Neteler and Mitasova, 2008). The *r.sun* program works in two modes. In the first mode, it calculates a solar incidence angle (degrees) and solar irradiance values (W m^{-2}) for the set local time. In the second mode, daily sums of solar radiation (Wh m^{-2} d^{-1}) are computed within a set day. The two modes can be used separately or combined to provide estimates for any desired time interval.

The solar incidence angle raster map is computed by specifying elevation raster, aspect raster, and slope steepness on a given day and at local time. There is no need to define latitude for locations with a known and defined projection/coordinate system. All input raster maps must be floating point raster maps. Null data in maps are excluded from the computation (also speeding it up), so that each output raster map will contain null data in cells according to all input raster maps.

The specified day is the number of the day in the general year where 1 January is day N° 1 and 31 December is 365. Time must be a local solar time using the decimal system, e.g., 9.5 (= 9 h 30 m AM). Setting the solar declination by user is an option to override the value computed by the internal routine for the day of the year. The value of geographic latitude can be set as a constant for the whole computed region or, as an option, a grid representing spatially distributed values over a large region. The geographic latitude must also be in the decimal system with positive and negative values for the northern and southern hemispheres, respectively. Similar in principle, the Linke turbidity factor and ground albedo can be set. Besides clear-sky radiation, the user can compute a real-sky radiation (beam, diffuse) with input raster maps defining the fraction of the respective clear-sky radiation reduced by atmospheric factors (e.g., cloudiness). The value is between 0 and 1. These coefficients can usually be obtained from long-term meteorological measurements.

Solar irradiation or irradiance raster maps are computed for a given day, latitude, elevation, slope, and aspect raster maps. For convenience, the output raster will output the sum of the three radiation components. The program uses the Linke atmosphere turbidity factor and ground albedo coefficient. Solar radiation maps for a given day are computed by integrating the relevant irradiance between the sunrise and sunset times for that day. The default step value is 0.5 h. Larger steps (e.g., 1.0 to 2.0) can speed up calculations but produce less reliable results. The output units are in Wh per square meter per given day (Wh m^{-2} d^{-1}).

The map history files are generated and contain the following parameters used in the computation: Solar constant 1367 W m^{-2}, extraterrestrial irradiance on a plane perpendicular to the solar beam (W m^{-2}), day of the year; declination (radians), decimal hour (mode 1 only), sunrise and sunset (min-max) over a horizontal plane, daylight length, geographic latitude (min-max), Linke turbidity factor (min-max), and ground albedo (min-max).

The user can employ a shell script with variable days to compute radiation for some time interval within the year (e.g., vegetation or winter period). Elevation, aspect, and slope input values should not be reclassified into coarser categories because this could lead to incorrect results. The *r.sun* model generates estimates of global solar radiation for clear-sky conditions. Overcast solar radiation can be calculated from the clear-sky values by applying a factor that parameterizes attenuation caused by cloudiness. The clear-sky index (K_c) represents the ratio between global solar radiation under overcast (G_h) and cloud-free (G_{hc}) conditions on a horizontal surface; its values range between 0.25 and 1.00:

$$K_c = G_h / G_{hc} \quad [2]$$

In addition to the *r.sun* model, there are several other mechanistic models that predict solar radiation (Ball *et al*.,

2004). To predict solar radiation, mechanistic models start calculating the extraterrestrial radiation and then reduce this value through some modifiers related to the day of the year, distance from the atmosphere to the ground, and air composition (e.g., dust, aerosols, and water). The extraterrestrial radiation (R_a, MJ m^{-2} d^{-1}) can be calculated for any given day of the year and latitude according to equations from Duffie and Beckman (1980).

$$R_a = \left(\frac{24*60}{\pi}\right) G_{sc} d_r [\omega_s \sin\delta \sin\phi + \cos\phi \cos\delta \sin\omega_s] \quad [3]$$

where G_{sc} = Solar constant = 0.082 [MJ m^{-2} min^{-1}]; d_r = correction for eccentricity of Earth's orbit around the sun on day i of the year:

$$d_r = 1 + 0.033\cos\left(\frac{2\pi}{365} i\right) \quad [4]$$

ω_s = sunrise hour angle (radians):

$$\omega_s = \cos^{-1}(-\tan\phi\tan\delta) \quad [5]$$

δ = declination of the sun above the celestial equator in radians on day i of the year:

$$\delta = 0.409\sin\left(\frac{2\pi}{365} i - 1.39\right) \quad [6]$$

ϕ = latitude in radians converted from latitude (L) in degrees:

$$\phi = \frac{\pi * L}{180} \quad [7]$$

With this calculation, we can obtain the incoming solar radiation on the ground (R_s):

$$R_s = R_a * T_t \quad [8]$$

where R_s is the solar radiation at the Earth's surface (MJ m^{-2} d^{-1}), R_a is the extraterrestrial radiation, and T_t is the atmospheric transmissivity.

Different models have been developed to calculate T_t, which are mostly based on empirical coefficients, temperature differentials, cloudiness, or daily sunshine hours (Ball *et al*., 2004). For instance, Hargreaves and Samani (1982) developed a simple model for estimating R_s. They proposed that T_t for a given day was proportional to the square root of the difference between maximum temperature (T_{max}) and minimum temperature (T_{min}). Using this work, Annandale *et al*. (2002) proceed to modify the model to include a correction for altitude (z, in [m]) such that:

$$T_t = k_{RS}\,(1+2.7E{-}5z)(T_{max} - T_{min})^{0.5} \quad [9]$$

where k_{RS} = adjustment coefficient for interior or coastal regions, and z = altitude (m). The adjustment coefficient k_{RS} is 0.16 for interior locations where a land mass dominates and air masses are not strongly influenced by a large water body. It is 0.19 for coastal locations on or adjacent to the coast of a large land mass and where air masses are influenced by a nearby water body. Altitude is an input parameter linked to a particular weather station.

Another alternative method of estimating T_t was developed by Bristow and Campbell (1984), where transmissivity was calculated as follows:

$$T_t = A[1.0{-}\exp(-B(T_{max} - T_{min})^C)] \quad [10]$$

where T_t is atmospheric transmittance, A is the maximum atmospheric transmittance expected at the site elevation (location characteristic that also depends on pollution), (T_{max} - T_{min}) is the daily range of temperature, and B and C are empirical coefficients when T_t reaches the maximum atmospheric transmittance (A) based on the daily temperature range. Values of these coefficients are 0.7 for A, between 0.004 and 0.010 for B, and 2.4 for C (Meza and Varas, 2000). The same authors adjusted site specific values for B in different locations in Chile.

Thornton and Running (1999) developed a sensitivity analysis for estimating coefficients of different sites in North America. These adjustments improved the quality of daily estimates to within ± 2.4 MJ m^{-2} d^{-1} at 40 sites with different soil and climatic conditions.

The aim of this paper is to estimate monthly solar radiation for the central regions of Chile using the *r.sun* model and to compute the three components of potential global solar radiation for clear-sky and overcast conditions. Specific objectives are: a) to evaluate methods based on weather station data to predict solar radiation for the study area; b) to evaluate the performance of these models and *r.sun* for 15 sites representing a range of climatic, elevation, and geographic locations.

The present work was initiated to develop a more robust approach for estimating and validating solar radiation estimates and provide surface maps with monthly estimates of solar radiation that can be used as input into process-based growth models.

MATERIALS AND METHODS

The study area included the south-central region of Chile located between 34°43' S and 40°36' S (Figure 1). The landscape includes the Coastal Range (mean elevation 550 m), the Central Valley, and the Andes Mountains foothills. The height of the Coastal Range greatly influences the Central Valley's climate (Santibáñez, 2003). There are 224 weather stations within our study area that record hourly precipitation and temperature data. Few stations (15) have global radiation measurements, and 11 stations make observations of cloudiness (oktas), which are measured three times a day (0800, 1400, and 2000 h).

For interpolation processes, we used a Digital Elevation Model (DEM) obtained from a forestry company in Chile (originally from the Shuttle Radar Topographic Mission, SRTM). To speed up calculations and because cloudiness data were at a low resolution, the DEM's spatial resolution was decreased to 500 m. Slope and aspect maps were obtained with the GRASS open source GIS tool (Neteler and Mitasova, 2008).

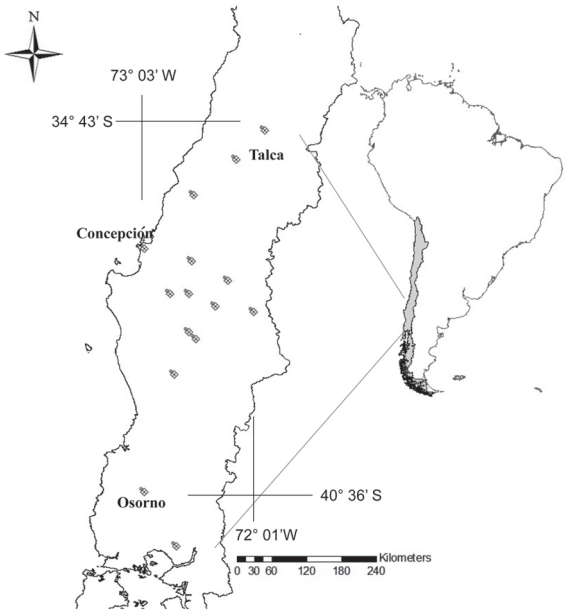

Figure 1. Research area in Chile, including weather stations with solar radiation sensors.

All raster data were integrated in GIS by Universal Transverse Mercator projection (World Geodetic System of 1984 datum zone 18 S). The raster resolution was 500 × 500 m^2. The ground albedo was considered as a constant 0.2.

With the *r.sun* model, we estimated clear-sky global radiation for a horizontal surface following these steps (Figure 2):

a. Obtaining Linke turbidity index (T_{LK}) data and spatial interpolation by Spline procedures (Mitasova and Mitas, 1993). Products are monthly raster maps (500 m spatial resolution) for the research area. We employed the *v.vol.rst* procedure in GRASS. In order to incorporate the topography (aspect and slope), we applied the digital elevation model with the same spatial resolution.

b. Construction of clear-sky map by means of the *r.sun* model (Suri and Hofierka, 2004). We run the model with a script in GRASS.

c. Calculation and spatial interpolation (Spline) of clear-sky index (0 to 1) and computation of monthly raster maps for global solar radiation on a horizontal surface. We used cloudiness data (oktas) from a Chilean network of weather stations, and we generated monthly raster maps for the clear-sky index.

d. Generation of monthly raster maps for overcast irradiation. These are the result of multiplying clear-sky irradiation by the clear-sky index.

Linke turbidity is an index that represents the amount of aerosols and dust in the atmosphere (Diabate *et al*., 2003). This index varies seasonally and spatially, especially around more industrialized areas. However, there is a global network of observations, and it is possible to obtain adequate values for different places around the world.

In the study area, monthly values of Linke turbidity were obtained for 185 spatially-distributed locations from the global database (Remund *et al*., 2003) available at SoDa service (Wald, 2000), which has reliable data available. The position of input points is defined with x, y,

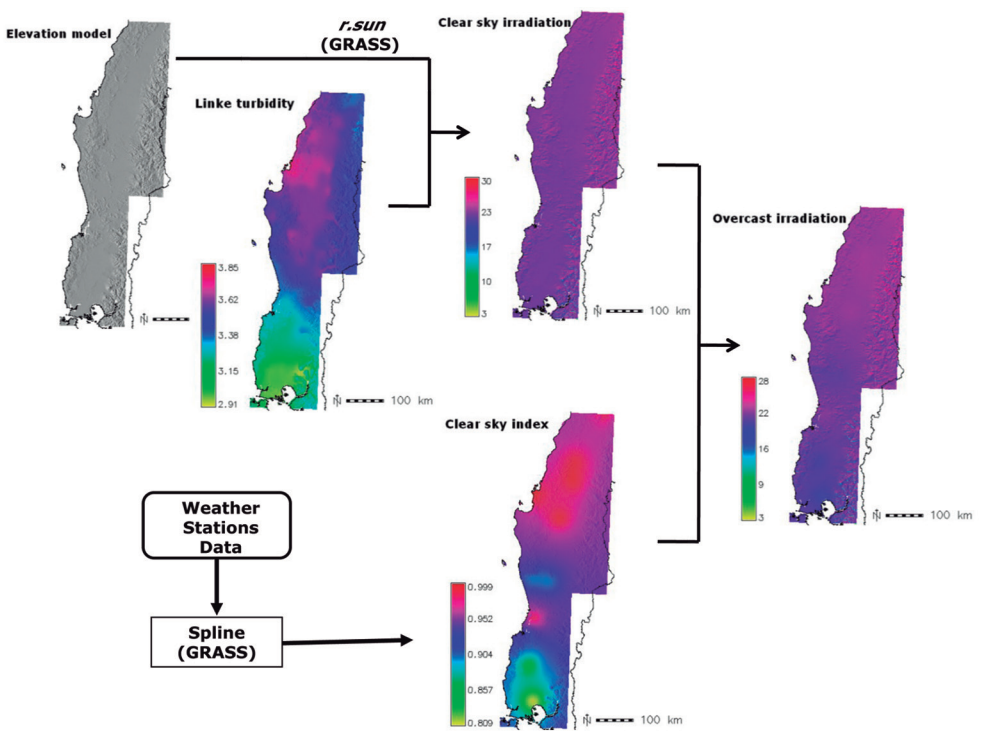

Figure 2. Activity sequence diagram for horizontal irradiation calculation.

and z values where z represents the elevation derived from the digital terrain model. We used the *v.vol.rst* procedure in GRASS GIS (see *v.vol.rst* manual page, Neteler and Mitasova 2008) and Mitasova and Mitas (1993). With this methodology, 12 monthly T_{LK} value raster maps were prepared (Figure 3). The interpolated results are very sensitive to the correct selection of parameters for tension, smoothing, and z-value conversion factors.

The *r.sun* model was parameterized for Chilean conditions with the slope, aspect, Linke turbidity, and cloudiness characteristics. A 0.5 h time step was considered satisfactory for daily solar radiation estimates. Declination values for each month were set according to the *r.sun* model at the middle of the month (15th day). The distance for the shadowing calculation was set to 0.7 and the albedo value to 0.2.

The clear-sky index (K_c) was calculated from a subset of daily and monthly measurements of oktas in the study area. In order to increase the original number of spatial locations with cloudiness (oktas), we fitted linear regressions between oktas against rainfall, minimum and maximum temperature, and elevation for 78 spatially-distributed locations. These monthly linear models exhibited strong R^2 (> 0.7) and also statistical significance for the parameters of each model ($\alpha = 0.05$). From these okta values, we obtained the K_c index for every month according to the models proposed by Kasten and Czeplak (1980), and we built monthly raster maps of cloud indices. The Kasten and Czeplak model has the following empirical equation:

$$K_c = 1 - 0.75\left(\frac{C}{8}\right)^{3.4} \qquad [11]$$

where C is cloudiness expressed in oktas.

Following a procedure similar to the Linke turbidity interpolation, we employed *v.vol.rst* for spatial interpolation of the clear-sky solar irradiation (Figure 4). To obtain monthly values, we imposed the specific calculation for the 15th day of each month from January to December in the *r.sun* model.

For each set of simulated (S_i) and observed (O_i) values, we evaluated the root mean squared error (RMSE), the intercept and slope coefficients of the linear relation between predicted and observed data, and the coefficient of determination. We calculated R_s for 15 representative sites of gradient (North to South) in order to compare the Hargreaves-Samani (HS), Bristow-Campbell (BC), and *r.sun* models (Table 1).

$$RMSE = \sqrt{\sum_{i=1}^{n} \frac{\left(S_i - O_i\right)^2}{n}} \qquad [12]$$

The best model should have r^2 close to 1, RMSE close to zero, and the intercept and slope not significantly different from 0 and 1, respectively. We compared a total of 180 observed-simulated values (n = 15 locations × 12 months).

We had observations of global solar radiation since 1997 for these locations. We included elevation for our calculations obtained from the DEM. Values of R_a were calculated for the 15th day of each month by standard geometric procedures, and transmissivity (T_t) was calculated by the specific procedures for the HS and BC models. We obtained the global radiation (R_s) for each location with both values. We calculated R_a, T_t, and R_s for any location (latitude and elevation) and for any day of the year (1 to 365). Climatic data (T_{max} and T_{min}) were

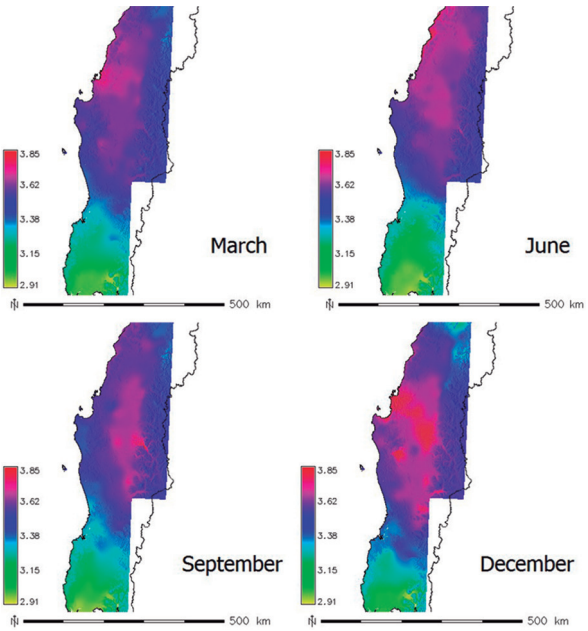

Figure 3. Linke turbidity maps of the study area for seasonal representative months in autumn (March), winter (June), spring (September), and summer (December).

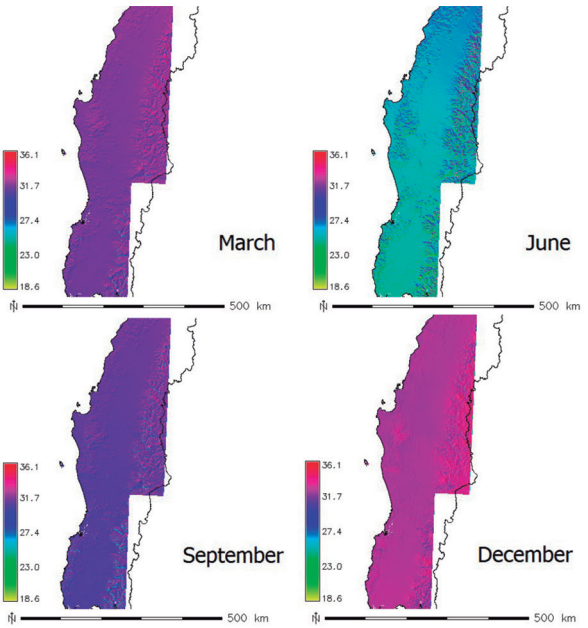

Figure 4. Monthly means of clear-sky solar irradiation area for representative seasonal months in autumn (March), winter (June), spring (September), and summer (December).

Table 1. Locations for solar irradiation model evaluation.

Station	S lat (°)	W long (°)	Altitude (m)
Curicó	-35.0	-71.2	225
Talca	-35.4	-71.7	129
Cauquenes	-36.0	-72.3	145
Rucamanqui	-37.3	-71.8	356
Colicheu	-37.0	-72.4	147
Los Ángeles	-37.5	-72.4	130
Concepción	-36.8	-73.1	12
Santa Bárbara	-37.7	-72.0	410
Nacimiento	-37.5	-72.7	107
Angol	-37.8	-71.4	75
Ercilla	-38.1	-72.4	250
Victoria	-38.2	-72.3	348
Temuco	-38.8	-72.6	114
Osorno	-40.6	-73.1	65
Puerto Montt	-41.4	-72.6	85

obtained from different weather station networks in the research area. We employed mean values for the last 10 yr of observations.

Analysis was performed with SAS (v. 9.3, SAS Institute, Cary, North Carolina, USA). Significant terms were obtained with $P < 0.05$.

RESULTS AND DISCUSSION

We determined monthly global solar radiation for horizontal surfaces of the south-central region of Chile, which is shown in 500 m spatial resolution raster maps. For *r.sun* results, Figure 4 (clear-sky solar radiation) and Figure 5 (overcast solar radiation) show four representative months (March, June, September, and December) in order to include low and high temperatures and vegetation development. Values varied during the year and were very low during the winter season (June).

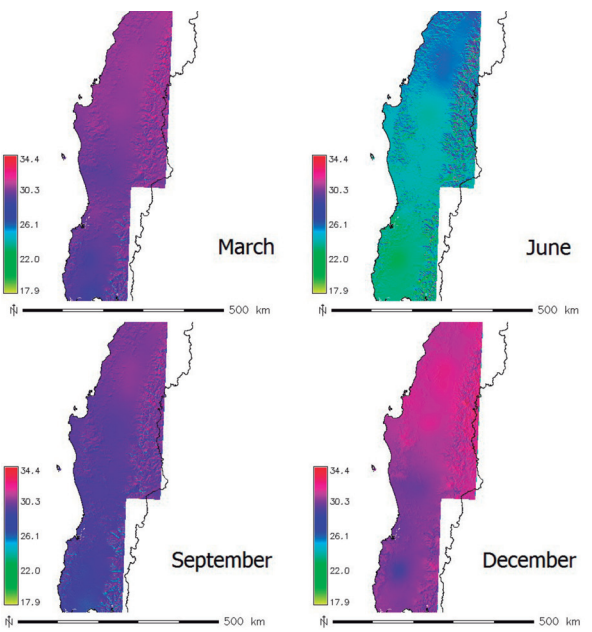

Figure 5. Monthly means of overcast solar irradiation area for representative seasonal months in autumn (March), winter (June), spring (September), and summer (December).

Summer season (December) values were the highest and fall (March) and spring (September) season values were intermediate. Clouds are more prevalent during the spring and fall seasons, especially on the coast and in the South. In the North, clouds are more prevalent during the winter season. The lack of cloudiness data in this area could be improved by remote sensing analysis (e.g., MODIS satellite).

The clear-sky solar radiation values show a strong north-south gradient as well as the influence of the Coastal and Andes Ranges. Maximum values of 30 to 34 MJ m^{-2} d^{-1} are more frequent in the North (summer). Minimum values of 4 to 6 MJ m^{-2} d^{-1} are common in the South during the winter season. According to K_c (clear-sky index), we can see a relevant effect on the winter season and also a north-south and Pacific Ocean to Andes Mountains effect. Maximum values of 34.3 MJ m^{-2} d^{-1} were obtained during the summer season (December). High elevations and north sides of the hills had high global solar radiation values. Southern exposures had lower values than northern ones. Comparing measured and predicted values of daily global radiation shows that these values are aligned along the 1:1 line as shown in Figures 6, 7, and 8.

The observed and simulated results were strongly correlated ($r^2 > 0.85$) for all the models (Table 2) with high slope coefficients and low RMSE. Estimates with BC and

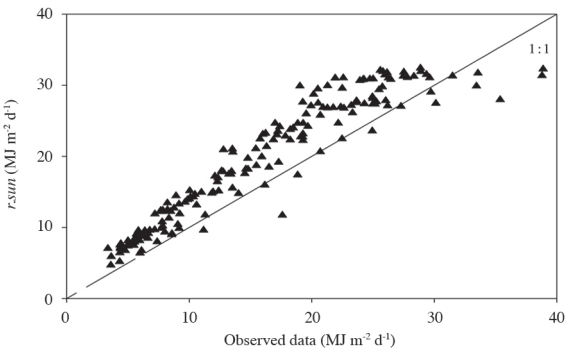

Figure 6. Observed and estimated mean monthly global solar irradiation using *r.sun* model. (Symbols represent data from 15 different weather stations).

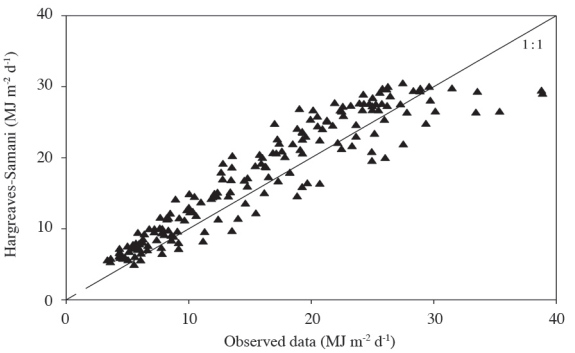

Figure 7. Observed and estimated mean monthly global solar irradiation using Hargreaves-Samani model. (Symbols represent data from 15 different weather stations).

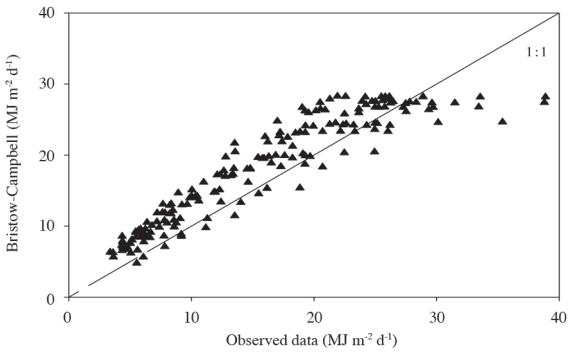

Figure 8. Observed and estimated mean monthly global solar irradiation using Bristow-Campbell model. (Symbols represent data from 15 different weather stations).

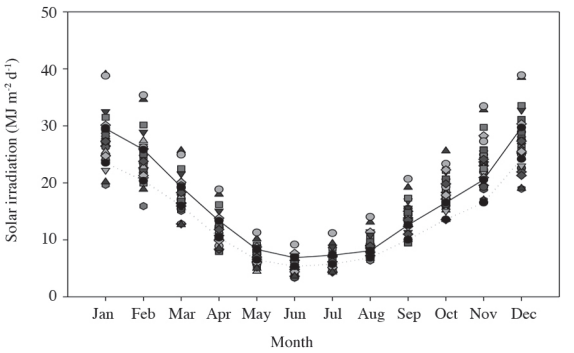

Figure 9. Global overcast sky solar irradiation on the study area. (Symbols represent observations from 15 locations and the solid line represents the mean from the *r.sun* model).

Table 2. Summary of statistical performance of Hargreaves-Samani (HS), Bristow-Campbell (BC), and *r.sun* models to predict irradiation at 15 sites in Chile. Monthly values of predicted irradiation were regressed against monthly mean values of observed irradiation (n = 180).

	Model		
Estimator	*r. sun*	Hargreaves-Samani	Bristow-Campbell
Intercept	3.90	3.11	5.04
Slope	0.97	0.89	0.82
r^2	0.90	0.87	0.86
RMSE	4.41	3.81	3.29

RMSE: Root mean squared error.

HS models resulted in lower values of RMSE than with the *r.sun* model. The observed and simulated values of solar radiation across the 15 locations had means of 15.8, 19.2, 17.2, and 17.9 MJ m^{-2} yr^{-1} for observed, *r.sun*, HS, and BC models, respectively. The differences are higher in the *r.sun* model, especially in the extreme locations and the summer months.

Total annual measured global solar radiation has a mean value of 5862 MJ m^{-2} yr^{-1}. Talca has the highest value (6312 MJ m^{-2} yr^{-1}), and Puerto Montt, the most southern and coastal location, has the lowest value (4231 MJ m^{-2} yr^{-1}). On a monthly basis, total global radiation varied from about 26 to 30 MJ m^{-2} d^{-1} in December and January to minimum means around 4 to 6 MJ m^{-2} d^{-1} during mid-winter (June-July). This coincides with the rainfall peak during the winter season (May-August). We showed this variation in Figure 9 where we included total solar radiation estimated with the *r.sun* model as well as observed data.

As in the Bristow and Campbell model, the *r.sun* model performance exhibits value overestimation for the study area (Figure 6). However, there was a strong relationship between observed and estimated values for monthly data means with *r.sun*. During the summer season (November-March), there was a minimized cloudiness effect which was probably not considered in the model because of the lack of observations. In addition, a possible lack of accuracy in the observed data could affect these relationships. Further revision of calibration for solar radiation sensors in the weather stations would be necessary to improve the accuracy of these measurements. Some stations exhibited monthly values > 32 MJ m^{-2} d^{-1}, which are probably over the standard values observed for similar conditions.

In the North of the gradient, model performance was more closely adjusted to the real values than in the South. In the central area, model performance was fitted near real solar radiation values; however, there was low overestimation for the summer season (the highest values).

In the southern part of the study area, there was a high correlation between observed and predicted values. However, we should expect a slight overestimation because of the greater cloud effect at these latitudes (> 40° S), which was probably underrepresented.

Linear regressions between predicted values for different models are shown in Table 2. This analysis was developed for representative locations in the gradient included in this study. The Hargreaves-Samani model was corrected by the elevation for each specific location. The results in Figures 6 to 8 and Table 2 showed close values between predicted and observed mean monthly incoming solar radiation.

The *r.sun* model has been implemented in Europe and North Africa, and this analysis was explored for further applications in South America. A better estimate of the clear-sky index could improve model performance for cloudy areas or during the winter season. This paper shows the application under horizontal conditions; however, it is possible to easily calculate the inclined solar radiation for steep terrains. The model can be used under any slope or aspect conditions. This makes the approach useful at individual sites as well as across broad landscapes.

The use of the *r.sun* model illustrates the possibility of obtaining realistic and spatially explicit data for different geographic locations. This characteristic is relevant in process-based models generally used in agriculture and forestry crops. On the other hand, the lack of solar radiation measurements from weather stations limits the use of mechanistic models. Due to the extreme variability of site conditions in south-central locations of Chile, the

use of temperature data (T_{max} and T_{min}) from the weather stations to estimate solar radiation does not allow good estimates for specific areas, especially due to the scarcity of observations in isolated locations. The *r.sun* model is flexible enough to estimate solar radiation for any site condition and has advantages in terms of flexibility, spatially explicit results, and does not require climatic data.

For the whole area in general, the Hargreaves-Samani model had a very good performance in terms of standard errors. The next best estimates were with the *r.sun* model, especially in the central part of the research area. As previously noted, transmittance in the South could be improved through better cloudiness estimates. We used the Bristow-Campbell model in the same way as Meza and Varas (2000) did with the coefficients A = 0.7, B = 0.007, and C = 2.4. Moreover, we did not apply the Bristow-Campbell approach used by Coops *et al*. (2000) because it was fitted for special conditions in North America and did not work well under Chilean conditions. Meza and Varas (2000) used the standard model parameters and fitted a model in order to get the optimum B coefficient for some specific locations in Chile. Coops *et al*. (2000) adjusted specific models for A and B and suggested a C value of 1.5. Using the standard parameters of their adjustments did not improve the performance of the Bristow-Campbell model in our study.

In the *r.sun* model, underlying equations for diffuse radiation were implemented to reflect European climatic conditions, and it should be a possible source of higher estimation errors for regions like Chile. The Bristow Campbell (1984) and Hargreaves-Samani (1982) methods provided very good estimates for specific locations (low standard errors), which represent advantages for further use in a specific location. Our estimates are closely related to those previously found by Meza and Varas (2000).

There are several opportunities to improve the quality of our model by using better cloud information. The lack of cloudiness data for the study area was improved through a linear regression adjusted for every month. Independent variables for oktas were rainfall, elevation, and maximum and minimum temperatures.

Further improvements need to be made through better cloudiness measurements with satellite images, such as MODIS. The results of this model could be easily connected to biological process models for tree growth modeling.

CONCLUSIONS

We calculated and built raster maps for monthly horizontal solar radiation for the south-central region of Chile. The *r.sun* model demonstrated very good performance for the site conditions.

It was possible to estimate monthly global solar radiation using the Bristow-Campbell and Hargreaves-Samani models, both based on meteorological data. The performance of these methods was closely associated with the *r.sun* model when they were validated for independent data from automatic weather stations.

The *r.sun* model, adjusted for Chile, represents a new opportunity to estimate solar radiation for any location inside the study area, especially due to the lack of weather stations and, even more, the lack of solar radiation sensors.

ACKNOWLEDGEMENTS

We acknowledge the permission given by Forestal Mininco and Modelo Nacional de Simulación de Pino Radiata to publish data and the results of our analyses. The senior author acknowledges the support of the Forest Productivity Cooperative at NCSU and the Center of Advanced Forestry Systems (CAFS) that allowed him to pursue scientific objectives in his work. We also thank Dr. Marcelo Miranda and Catalina Gerstmann from the Pontificia Universidad Católica de Chile for providing additional climatic data.

Estimación de radiación solar mensual en la zona centro sur de Chile. La radiación solar es un componente clave en los modelos basados en procesos. La cantidad de esta energía depende de la ubicación, época del año, y también de las condiciones atmosféricas. Varias ecuaciones y modelos han sido desarrollados para diferentes condiciones, utilizando datos históricos de las redes de estaciones meteorológicas o de las mediciones por satélite. Sin embargo, las estimaciones de la radiación solar son demasiado locales con estaciones meteorológicas, o con una resolución muy gruesa cuando se trabaja con satélites. En el presente estudio se estimó radiación solar global mensual para la región centro sur de Chile mediante el uso del modelo *r.sun* y se validó con observaciones de estaciones meteorológicas automáticas. Se analizó el desempeño de los resultados de la irradiación global con los modelos Hargreaves-Samani (HS) y Bristol-Campbell (BC). Las estimaciones del modelo calibrado *r.sun* explican un 89% de la varianza (r^2 = 0.89) en valores medios mensuales observados. El modelo se comportó muy bien para una amplia zona de las condiciones de Chile, comparados con los modelos HS y BC. Nuestras estimaciones de la radiación global utilizando el modelo *r.sun* podrían ser mejoradas aún más con una posterior calibración a partir de observaciones y una mejor estimación de la nubosidad en la medida que estén disponibles. Con procedimientos adicionales, el modelo *r.sun* podría ser utilizado para proporcionar estimaciones espaciales de la radiación solar diaria, semanal, mensual, y anual.

Palabras clave: Radiación solar, modelo *r.sun*.

LITERATURE CITED

Almeida, A., and J.J. Landsberg. 2003. Evaluating methods of estimating global radiation and vapor pressure deficit using a dense network of automatic weather stations in coastal Brazil. Agricultural and Forest Meteorology 118:237-250.

Almeida, A.C., J.J. Landsberg, and P.J. Sands. 2004. Parameterisation of 3-PG for fast growing *Eucalyptus grandis* plantations. Forest Ecology and Management 193:179-295.

Annandale, J.G., N.Z. Jovanic, N. Benade, and R.G. Allen. 2002. Software for missing data error analysis of Penman-Monteith reference evapotranspiration. Irrigation Science 21:57-67.

Ball, R.A., L.C. Purcell, and S.K. Carey. 2004. Evaluation of solar radiation prediction models in North America. Agronomy Journal 96:391-397.

Battaglia, M., P. Sands, D. White, and D. Mummery. 2004. CABALA: a linked carbon, water and nitrogen model of forest growth for silvicultural decision support. Forest Ecology and Management 193:251-282.

Bindi, M., and P. Miglietta. 1991. Estimating daily global radiation from air temperature and rainfall measurements. Climate Research 1:117-124.

Bristow, K.L., and G.S. Campbell. 1984. On the relationship between incoming solar radiation and daily maximum and minimum temperature. Agricultural and Forest Meteorology 31:159-166.

Cano, D., J.M. Monget, M. Albuisson, H. Guillard, N. Regas, and L. Wald. 1986. A method for the determination of the global solar radiation from meteorological satellite data. Solar Energy 37:31-39.

Coops, N.C., R.H. Waring, and J.J. Landsberg. 1998. Assessing forest productivity in Australia and New Zealand using a physiologically-based model driven with averaged monthly weather data and satellite-derived estimates of canopy photosynthetic capacity. Forest Ecology and Management 104:113-127.

Coops, N.C., R.H. Waring, and J.B. Moncrieff. 2000. Estimating mean monthly incident solar radiation on horizontal and inclined slopes from mean monthly temperatures extremes. International Journal of Biometeorology 44:204-211.

Diabate, L., G. Moussu, and L. Wald. 1989. Description of an operational tool for determining global solar radiation at ground using geostationary satellite images. Solar Energy 42:201-207.

Diabate, L., J. Remund, and L. Wald. 2003. Linke turbidity factors for several sites in Africa. Solar Energy 75:111-119.

Díaz, D., L. Morales, G. Castellaro, and F. Neira. 2010. Topoclimatic modeling of thermopluviometric variables for the Bío Bío and La Araucanía Regions, Chile. Chilean Journal of Agricultural Research 70:604-615.

Duffie, J.A., and W.A. Beckman. 1980. Solar engineering of thermal processes. Wiley Inter-Science, New York, USA.

ESRA. 2000. European Solar Radiation Atlas. 4th ed. Includ. CD-ROM. Greif, J., and K. Scharmer (eds.) Commission of the European Communities, Presses de l'Ecole des Mines de Paris, Paris, France.

Garatuza-Payan, J., R.T. Pinker, W.J. Shuttleworth, and C.J. Watts. 2001. Solar radiation and evatranspiration in northern Mexico estimated from remotely sensed measurements of cloudiness. Hydrological Sciences Journal 46:465-478.

Hargreaves, G.H., and Z.A. Samani. 1982. Estimating potential evapotranspiration. Journal of Irrigation and Drainage Engineering 108:225-230.

Hofierka, J., and M. Suri. 2002. The solar radiation model for Open Source GIS: implementation and applications. Proceedings of the Open Source Free Software GIS-GRASS users conference 2002 – Trento, Italy. 11-13 September 2002. University of Trento, Department of Civil and Environmental Engineering, Trento, Italy.

Kasten, F., and G. Czeplak. 1980. Solar and terrestrial radiation dependent on the amount and type of cloud. Solar Energy 24:177-189.

Kermel, F. 1988. Estimating hourly all-sky irradiation components from meteorological data. Journal of Applied Meteorology 27:157-163.

Landsberg, J.J., and R.H. Waring. 1997. A generalized model of forest productivity using simplified concepts of radiation-use efficiency, carbon balance and partitioning. Forest Ecology and Management 95:209-228.

Lefevre, M., L. Wald, and L. Diabate. 2007. Using reduced data sets ISCCP-B2 from the Meteosat satellites to asses surface solar irradiance. Solar Energy 81:240-253.

Linke, F. 1922. Transmissionkoeffizient und Trubungsfaktor. Beitraege zur Physik der Atmosphaere 10:91-103.

McMurtrie, R.E., D.A. Rock, and F.M. Kelliher. 1990. Modelling the yield of *Pinus radiata* on a site limited by water and nitrogen. Forest Ecology and Management 30:381-413.

Meza, F., and E. Varas. 2000. Estimation of mean monthly solar global radiation as a function of temperature. Agricultural and Forest Meteorology 100:231-241.

Mitasova, H., and L. Mitas. 1993. Interpolation by regularized spline with tension: I. Theory and implementation. Mathematical Geology 25:641-655.

Muneer, T., M.S. Gul, and J. Kubie. 2000. Models for estimating solar radiation and illuminance from meteorological parameters. Journal of Solar Energy Engineering 122:146-153.

Neteler, M., and H. Mitasova. 2008. Open Source GIS: A GRASS GIS approach. 3rd ed. The International Series in Engineering and Computer Science Vol. 773. 406 p. Springer, New York, USA.

Remund, J., L. Wald, M. Lefevre, T. Ranchin, and J. Page. 2003. Worlwide Linke turbidity information. Proceedings of ISES Solar World Congress, Goteborg, Sweden.

Romero, L.F., S. Tabik, J.M. Vias, and E.L. Zapata. 2008. Fast clear-sky solar irradiation computation for very large digital elevation models. Computer Physics Communications 178:800-808.

Sands, P.J., and J.J. Landsberg. 2002. Parameterisation of 3-PG for plantation grown *Eucalyptus globulus*. Forest Ecology and Management 163:273-292.

Santibáñez, F. 2003. Atlas climático de Chile. Universidad de Chile, Santiago, Chile.

Stape, J.L., M.G. Ryan, and D. Binkley. 2004. Testing the utility of the 3-PG model for growth of *Eucalyptus grandis x urophylla* with natural and manipulated supplies of water and nutrients. Forest Ecology and Management 193:219-234.

Suri, M., and J. Hofierka. 2004. A new GIS-based solar radiation model and its application to photovoltaic assessments. Transactions in GIS 8:175-190.

Tickle, P.K., N.C. Coops, and S.D. Hafner. 2001. Assessing forest productivity at local scales across a native eucalypt forest using a process model, 3PG-SPATIAL. Forest Ecology and Management 152:275-291.

Thornton, P.E., and S.W. Running. 1999. An improved algorithm for estimating incident daily solar radiation from measurements of temperature, humidity, and precipitation. Agricultural and Forest Meteorology 93:211-228.

Wald, L. 2000. SODA: a project for the integration and exploitation of networked solar radiation databases. European Geophysical Society Meeting, XXV General Assembly, Nice, France. 25-29 April 2000.

Wang, Y.P., and P.G Jarvis. 1990. Description and validation of an array model- MAESTRO. Agricultural and Forest Meteorology 51:257-280.

Yilmaz, E., B. Cancino, and E. Lopez. 2007. Construction of a quadratic model for predicted and measured global solar radiation in Chile. Chinese Physics Letters 24:291-293.